Int. J. Heat Mass Transfer. Vol. 2, pp. 121–135. Pergamon Press 1961, Printed in Great Britain.

FREE-CONVECTION SIMILARITY FLOWS ABOUT TWO-DIMENSIONAL AND AXISYMMETRIC BODIES WITH CLOSED LOWER ENDS

WILLIS H. BRAUN, SIMON OSTRACH* and JOHN E. HEIGHWAY
Lewis Research Center,
National Aeronautics and Space Administration, Cleveland, Ohio

(*Received* 1 *April* 1960; *revised* 4 *June* 1960)

Abstract—Families of bodies with closed lower ends are found that have similar velocity and temperature profiles along their entire extents. Several two-dimensional and axisymmetric bodies are presented, and growth of boundary-layer thickness and velocity along the surfaces, as well as the heat transfer, are computed for a wide range of Prandtl numbers. The effect of variable wall temperature is discussed, and the extension of the results to nonsimilar bodies is indicated.

Résumé—Il a été trouvé que des familles de corps ayant leur extrémité inférieure fermée avaient des profils de vitesse et de température semblables sur toute leur longueur. Plusieurs corps de révolution et bidimensionnels sont présentés; l'épaississement de la couche limite et la vitesse le long de leur surface, aussi bien que la transmission de chaleur, ont été calculées pour un grand domaine de nombres de Prandtl. L'effet d'une température de paroi variable est discuté et l'extension des résultats à des corps différents est indiquée.

Zusammenfassung—Es zeigt sich, dass es Familien von Körpern mit geschlossenen unteren Enden gibt, die ähnliche Geschwindigkeits- und Temperaturprofile über ihre ganze Erstreckung besitzen. Einige zweidimensionale und achsensymmetrische Körper werden mitgeteilt und das Anwachsen der Grenzschichtdicke und der Verlauf der Geschwindigkeit längs der Oberfläche sowie die Wärmeübertragung für einen grossen Bereich der Prandtlzahl berechnet. Die Wirkung einer veränderlichen Wandtemperatur wird diskutiert und die Ausdehnung der Ergebnisse auf nichtähnliche Körper angezeigt.

Аннотация—Установлено, что группа тел с закрытыми нижними концами имеет подобные профили скоростей и температур на всем их протяжении. Рассматриваются несколько двухразмерных и осесимметричных тел, для которых в широком диапазоне чисел Прандтля подсчитываются изменение толщины пограничного слоя и скорости вдоль поверхности, а также коэффициент теплообмена. Обсуждается вопрос о влиянии переменной температуры стенки и указывается возможность распространить полученные результаты на другие (не подобные) тела.

NOMENCLATURE

A,	constant;
a, b, c, d,	constants;
$E(\alpha, \varphi)$,	elliptic integral of second kind;
$F(\alpha, \varphi)$,	elliptic integral of first kind;
$F(\eta)$,	stream function profile;
$f(x)$,	velocity growth function;
G,	acceleration due to gravity;
$g(x)$,	boundary-layer thickness function;
$H(\eta)$,	temperature profile;
$h(x)$,	temperature growth function;
k,	heat conductivity;
L,	characteristic length;
M,	boundary-layer parameter for variable temperature case;
m,	body-shape parameter;
n,	temperature-difference index;
Nu,	Nusselt number;
O,	origin;
Pr,	Prandtl number;
$R_0(X)$,	body radius;
$r(x)$,	dimensionless body radius;

* Now, Professor of Mechanical Engineering, Case Institute of Technology, Cleveland, Ohio.

r_∞, dimensionless radius of $m = \infty$ body;
Ra, Rayleigh number;
s, variable of integration;
T, temperature;
T_∞, temperature far from body;
t, dimensionless temperature difference;
U, V, velocity components along and normal to body, respectively;
V^*, characteristic velocity;
X, Y, co-ordinates along and normal to body surface;
x, y, dimensionless co-ordinates;
Z, axial co-ordinate;
z, dimensionless axial co-ordinate;
α, thermal diffusivity;
β, coefficient of thermal expansion;
δ, dimensionless boundary-layer thickness;
ζ, boundary-layer similarity co-ordinate;
η, unscaled boundary-layer similarity co-ordinate;
θ, half angle of cone;
ν, kinematic viscosity;
ρ, radius of curvature;
φ, parameter angle;
ψ, dimensionless stream function.

Subscripts:
max, upper extremity of body;
w, wall condition;
X, Y, x, y, partial differentiation (except G_X and G_Y).

INTRODUCTION

In forced convection, the concept of similarity flows has been thoroughly discussed. Falkner and Skan [3] made the primary investigation on a class of bodies that have similar velocity profiles in the boundary layer over their entire extents. The velocity at the edge of the boundary layer varies as some power of the distance from the leading edge or stagnation point.

The analogous discussion of similar natural convection flows was begun by Schuh [8]. He discussed the flow over a two-dimensional body having everywhere finite curvature and a boundary-layer of constant thickness. Later, Merk and Prins [5] developed the general relations describing axisymmetric bodies as well. They showed that the cone is one axisymmetric body having a similarity flow.

In this paper, we develop a considerable number of the two-dimensional bodies and two more of the axisymmetric bodies. We limit ourselves to bodies with closed lower ends. The upper ends are open and usually the bodies are only of finite extent. The boundary-layer flows on these bodies are solved approximately by an integral method over a wide range of Prandtl numbers in order to show how the heat transfer varies along bodies and from body to body. Several numerical solutions for air are also presented. Finally, extensions to variable wall temperature and non-similar bodies are made. Although the flows are here treated as external to the bodies, the same formalism and solutions apply to internal boundary layers.

NATURAL CONVECTION OVER TWO-DIMENSIONAL CLOSED-END BODIES

Similarity conditions

Consider the symmetric body shown in cross section in sketch (a). Its contour is described by

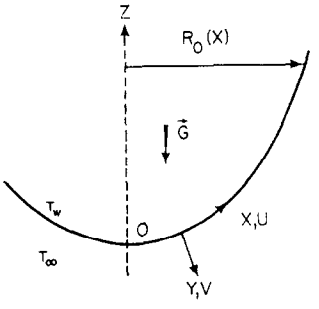

Sketch (a)

the radius from the axis $R_0(X)$, where X is the surface co-ordinate measured from the origin O. The co-ordinate Y is normal to the surface. The components G_X and G_Y of the acceleration due to gravity in this system are, at the body surface,

$$G_X = G\sqrt{[1 - (R_0')^2]},$$

$$G_Y = GR_0'.$$

The equations governing the flow of a thin boundary layer on the surface are

$$U_X + V_Y = 0 \tag{1}$$

$$UU_X + VU_Y = \nu U_{YY} + G\sqrt{[1 - (R_0')^2]}\,\beta(T - T_\infty), \tag{2}$$

$$UT_X + VT_Y = \alpha T_{YY}. \tag{3}$$

In equation (2), β is the coefficient of thermal expansion.

Several simplifications have been incorporated into equations (1), (2) and (3). Curvature terms have been omitted under the assumption that the boundary-layer thickness is small compared with the local radius of curvature [4]. However, some of the bodies to be discussed have a vanishing radius of curvature at the tip and, therefore, the boundary-layer assumptions will not be valid there. In the case of liquids, the equations are limited to small values of the product $\beta(T - T_\infty)$ [7]. For gases, however, the equations apply for arbitrary temperature differences provided that the products of density by conductivity and density by viscosity are constant across the boundary layer [9]. Then $\beta = 1/T_\infty$ and the equations as presented are derived from the compressible-fluid equations by a Dorodnitzyn–Howarth transformation. Near the bottom of the body, there may be an extended region of nearly horizontal surface. Stewartson [10] has shown that a boundary-layer phenomenon of a different, but weaker, kind may appear under such conditions. However, only the usual (and presumably stronger) buoyancy-induced boundary layer is considered here. Lastly, it is assumed that the dissipation term may be omitted in the energy equation (3).

For convenience, we nondimensionalize the equation by introducing a characteristic length L, a characteristic velocity V^* to be determined later, and the temperature difference $T_w - T_\infty$, where T_w is the temperature at a station along the wall to be specified later. The dependent and independent variables become, by introducing a dimensionless stream function,

$$U = V^*\psi_y(x, y),\quad V = -V^*\psi_x(x, y),$$
$$T - T_\infty = (T_w - T_\infty)t\,(x, y),$$
$$X = Lx,\quad Y = Ly,\quad R_0(X) = Lr(x). \tag{4}$$

Equations (2) and (3) become

$$\psi_y\psi_{yx} - \psi_x\psi_{yy} = \frac{\nu}{V^*L}\psi_{yyy} + \frac{\beta(T_w - T_\infty)GL}{(V^*)^2}\sqrt{[1 - (r')^2]}\,t, \tag{5}$$

and

$$Pr(\psi_y t_x - \psi_x t_y) = \frac{\nu}{V^*L}\,t_{yy}. \tag{6}$$

We seek a similarity solution of the form

$$\psi = f(x)F(\eta),\quad \eta = y/g(x),\quad t = h(x)H(\eta) \tag{7}$$

and ask under what conditions, i.e. for what bodies, the partial differential equations (5) and (6) become ordinary equations for $F(\eta)$ and $H(\eta)$. The functions $F'(\eta)$ and $H(\eta)$ describe, respectively, the velocity and temperature-difference distributions across the boundary layer. The functions $g(x)$, $f(x)/g(x)$, and $h(x)$ represent the growth of boundary-layer thickness, velocity and temperature difference along the wall.

Substitution of equation (7) into (5) and (6) yields

$$\left(\frac{f}{g}\right)^2\left[\left(\frac{f'}{f} - \frac{g'}{g}\right)(F')^2 - \frac{f'}{f}FF''\right] = \frac{\nu}{V^*L}\,\frac{f}{g^3}F''' + \frac{\beta(T_w - T_\infty)GL}{(V^*)^2}\sqrt{[1 - (r')^2]}\,hH, \tag{8}$$

$$Pr\,fg\left(\frac{h'}{h}HF' - \frac{f'}{f}FH'\right) = \frac{\nu}{V^*L}H''. \tag{9}$$

If equations (8) and (9) are to reduce to ordinary equations in η alone, the following proportionalities must hold:

$$\frac{f'}{f} - \frac{g'}{g} \approx \frac{f'}{f},\quad f'g \approx 1,$$
$$f \approx g^3h\sqrt{[1 - (r')^2]},\quad \frac{h'}{h} \approx \frac{f'}{f}. \tag{10}$$

Constant wall temperature

If we restrict ourselves to the conditions of constant surface temperature, then

$$H(0) = 1,\quad h(x) = 1,\quad h' = 0. \tag{11}$$

The fourth of conditions (10) no longer applies. Furthermore, we may choose unity for the constants of proportionality in the second and third conditions, for it is easily shown that only a scaling of the variables F and η is involved. Thus, we are interested in finding body shapes satisfying

$$\frac{f'}{f} = m\frac{g'}{g}, \quad f'g = 1, \quad f = g^3\sqrt{[1-(r')^2]}, \tag{12}$$

subject to the condition, imposed by the symmetry of the body, that the velocity vanish at $x = 0$. The functions f and g are found to be

$$f = \left(\frac{m+1}{m}x\right)^{m/(m+1)}, \quad g = \left(\frac{m+1}{m}x\right)^{1/(m+1)}, \tag{13}$$

while the body contour is defined by

$$r' = \sqrt{\left[1-\left(\frac{m+1}{m}x\right)^{2(m-3)/(m+1)}\right]}. \tag{14}$$

Equations (13) and (14) are special forms of relations found by Merk and Prins [5].

For any value of the parameter m, the axial co-ordinate of any position x along the surface is given by

$$z = \frac{m}{2(m-1)}\left(\frac{m+1}{m}x\right)^{2(m-1)/(m+1)}. \tag{15}$$

From (14) and (15 the radius of curvature ρ is found to be defined by

$$\left.\begin{aligned}\frac{1}{\rho} &\equiv \sqrt{[(r'')^2+(z'')^2]} = \\ &\{(m-3)/m\}\Big/\left\{\left(\frac{m+1}{m}x\right)^{4/(m+1)}\times\right. \\ &\left.\sqrt{\left[1-\left(\frac{m+1}{m}x\right)^{2(m-3)/(m+1)}\right]}\right\}.\end{aligned}\right\} \tag{16}$$

Specific body shapes

In equation (14) it is apparent that negative powers of x within the radical result in imaginary values of r' near the origin. Consequently, there is a restriction on the body parameter m of the form

$$\frac{2(m-3)}{m+1} \geq 0 \tag{17}$$

which has the solutions

$$m \geq 3, \quad m \leq -1. \tag{18}$$

All values of the parameter m are thus available for constructing contours except the values

$$-1 \leq m < 3. \tag{19}$$

With positive powers of x occurring in the radical, it is necessary, also in order to keep r' real, to bound x:

$$0 \leq \frac{m+1}{m}x \leq 1. \tag{20}$$

Thus the bodies are limited in extent.

Integrals of (14), subject to the restriction of closed end bodies,

$$r(0) = 0, \tag{21}$$

are given below for several values of m:

$\underline{m = 3}$

$$r' = 0, \quad r = 0, \quad z = x. \tag{22}$$

This is simply the vertical flat plate.

$\underline{m = 19/5}$

$$\left.\begin{aligned}&0 \leq s = (24x/19)^{1/3} \leq 1, \\ r &= \frac{19}{8}\int_0^s s^2\sqrt{(1-s)}\,ds \\ &= \frac{38}{105}\left[1-\left(1+\frac{3}{2}s+\frac{15}{8}s^2\right)(1-s)^{3/2}\right], \\ z &= \frac{19}{28}s^{7/2}.\end{aligned}\right\} \tag{23}$$

$\underline{m = 13/3}$

$$\left.\begin{aligned}&0 \leq s = (16x/13)^{1/2} \leq 1, \\ r &= \frac{13}{8}\int_0^s s\sqrt{(1-s)}\,ds \\ &= \frac{13}{30}\left[1-\left(1+\frac{3}{2}s\right)(1-s)^{3/2}\right], \\ z &= \frac{13}{20}s^{5/2}.\end{aligned}\right\} \tag{24}$$

$\underline{m = 5}$

$$\left.\begin{aligned} &0 \le s = (6x/5)^{1/3} \le 1,\\ r &= \frac{5}{2}\int_0^s s^2\sqrt{(1-s^2)}\,ds\\ &= \frac{5}{8}\left\{-s(1-s^2)^{3/2} + \frac{1}{2}\left[s\sqrt{(1-s^2)} + \sin^{-1}s\right]\right\},\\ z &= \frac{5}{8}s^4. \end{aligned}\right\} \quad (25)$$

$\underline{m = 7}$

$$\left.\begin{aligned} &0 \le s = 8x/7 \le 1,\\ r &= \frac{7}{8}\int_0^s \sqrt{(1-s)}\,ds\\ &= \frac{7}{12}[1-(1-s)^{3/2}],\\ z &= \frac{7}{12}s^{3/2}. \end{aligned}\right\} \quad (26)$$

$\underline{m = 11}$

$$\left.\begin{aligned} &0 \le s = (12x/11)^{1/3} = \cos\varphi \le 1,\\ r &= \frac{11}{4}\int_0^s s^2\sqrt{(1-s^4)}\,ds\\ &= \frac{11}{10\sqrt{(2)}}\{\cos^3\varphi\sin\varphi\sqrt{(1-1/2\sin^2\varphi)}\\ &\quad + 2[E(45°, 90°) - E(45°, \varphi)]\\ &\quad - [F(45°, 90°) - F(45°, \varphi)]\},\\ z &= \frac{11}{20}(\cos\varphi)^5. \end{aligned}\right\} \quad (27)$$

$\underline{m = 15}$

$$\left.\begin{aligned} &0 \le s = (16x/15)^{1/2} \le 1,\\ r &= \frac{15}{8}\int_0^s s\sqrt{(1-s^3)}\,ds\\ &= \frac{45}{56}\left\{\frac{1-\sqrt{(3)}}{3^{1/4}}[F(75°, \varphi_l) - F(75°, \varphi)]\right.\\ &\quad + 2\cdot 3^{1/4}[E(75°, \varphi_l) - E(75°, \varphi)]\\ &\quad \left. - 2\cdot 3^{1/4}\left[\frac{\sin\varphi_l\sqrt{(1-k^2\sin^2\varphi_l)}}{1+\cos\varphi_l} - \frac{\sin\varphi\sqrt{(1-k^2\sin^2\varphi)}}{1+\cos\varphi}\right]\right\}\\ &\quad + \frac{15}{28}s^2\sqrt{(1-s^3)},\\ z &= \frac{15}{28}s^{7/2}\\ s &= \frac{1-\sqrt{(3)}+[1+\sqrt{(3)}]\cos\varphi}{1+\cos\varphi}\\ &0 \le \varphi \le \varphi_l = \cos^{-1}\frac{\sqrt{(3)}-1}{\sqrt{(3)}+1},\\ k &= \sin 75°. \end{aligned}\right\} \quad (28)$$

$\underline{m = \infty}$

$$\left.\begin{aligned} r &= \int_0^x \sqrt{(1-x^2)}\,dx\\ &= \frac{1}{2}[x\sqrt{(1-x^2)} + \sin^{-1}x],\\ z &= \frac{1}{2}x^2,\\ &0 \le x \le 1. \end{aligned}\right\} \quad (29)$$

Here $F(\alpha, \varphi)$ and $E(\alpha, \varphi)$ are the elliptic functions of the first and second kinds, respectively.

This is the body discussed in [8].

$m = -9$

$$
\left.
\begin{aligned}
&0 \le s = 8x/9 \le 1,\\
r &= \frac{9}{8}\int_0^s \sqrt{(1-s^3)}\,ds\\
&= \frac{27}{40}\,3^{-1/4}\,[F(75°, \varphi_l) - F(75°, \varphi)]\\
&\quad + \frac{9}{20}\,s\,\sqrt{(1-s^3)},\\
z &= \frac{9}{20}\,s^{5/2},\\
s &= \frac{1 - \sqrt{(3)} + [1 + \sqrt{(3)}]\cos\varphi}{1 + \cos\varphi},\\
&0 \le \varphi \le \varphi_l = \cos^{-1}\frac{\sqrt{(3)} - 1}{\sqrt{(3)} + 1}.
\end{aligned}
\right\} \quad (30)
$$

$m = -5$

$$
\left.
\begin{aligned}
&0 \le s = 4x/5 = \cos\varphi \le 1,\\
r &= \frac{5}{4}\int_0^s \sqrt{(1-s^4)}\,ds\\
&= \frac{5}{12}\sqrt{(2)}\,[F(45°, 90°) - F(45°, \varphi)]\\
&\quad + \frac{5}{12}\cos\varphi\sin\varphi\,\sqrt{(1+\cos^2\varphi)},\\
z &= \frac{5}{12}(\cos\varphi)^3.
\end{aligned}
\right\} \quad (31)
$$

$m = -1$

$$r = x, \quad z = 0. \qquad (32)$$

This is the case of the horizontal plane, for which the buoyancy-type boundary-layer flow vanishes identically. As remarked previously, however, another type of boundary-layer flow, which results from pressure differences set up by the temperature distribution, may be generated [10].

The body contours are shown in Fig. 1. All of the bodies have vanishing slope (dz/dr) at the origin, except for the vertical flat plate ($m = 3$). Nevertheless, for $m > 3$ the radius of curvature vanishes at the origin, and in this sense the bodies in this parameter range are pointed. Only the body defined by $m = \infty$ has a finite curvature at the origin, and it is, in this case, the characteristic length. For all $m \le -1$, $\rho(0) = \infty$; one may refer to these contours as flat bottomed. As anticipated, the bodies are limited in extent, with the exception of the vertical and horizontal plates. At their upper extremes the contours are parallel to the axis, i.e. vertical. The characteristic lengths are easily determined from the maximum vertical or surface co-ordinates to be

$$L = (m+1)X_{\max}/m = 2(m-1)Z_{\max}/m. \qquad (33)$$

In each particular case, a relation between the maximum radius and the characteristic length may also be found.

Reference to equations (13) shows how the velocity and boundary-layer thickness vary

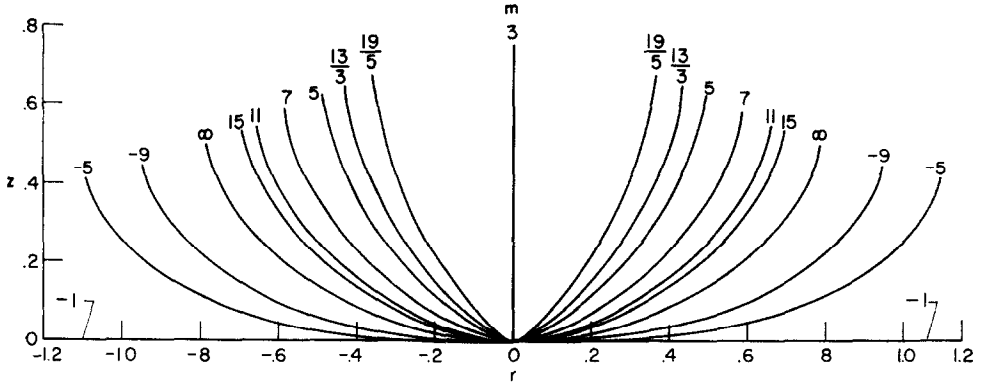

FIG. 1. Two-dimensional similarity bodies.

along the body wall in each case. For those bodies whose characteristic parameter m lies in the range $3 \leq m < \infty$ (pointed bodies), the stream function variation $f(x)$ and the boundary-layer thickness $g(x)$ increase like roots of x. The flow is qualitatively like that over the flat plate ($m = 3$). The round-nosed body ($m = \infty$) has a linearly increasing velocity ($f = x$) and constant boundary-layer thickness ($g = 1$). One thinks immediately of the Schlieren photographs of natural convection flow about a heated cylinder presented by Eckert [2], which show isotherms to be lines of nearly constant radius. The flat-bottomed contours ($m < -1$) have velocities varying as a power, greater than one, of x, and a boundary-layer thickness that varies according to a negative power of x. Consequently, the thickness grows without bound as one approaches the origin, and we must conclude that the assumption of a thin boundary layer is not valid there. The boundary-layer type solutions, which will be presented below, are then to apply only sufficiently far from the origin.

Variable wall temperature

Certain wall temperature variations are compatible with similarity solutions of the differential equations of motion (8), (9). To find these we choose the constants of proportionality in the second and third of equations (10) to be unity, and write

$$\frac{f'}{f} = M\frac{g'}{g}, \quad f'g = 1,$$

$$f = \sqrt{[1 - (r')^2]}\, g^3 h, \quad \frac{h'}{h} = n\frac{f'}{f}. \tag{34}$$

Here the parameter M takes the value m of the previous section when $n = 0$. The solution of this set is

$$\left.\begin{aligned} g &= \left(\frac{M+1}{M}x\right)^{1/(M+1)}, \\ f &= \left(\frac{M+1}{M}x\right)^{M/(M+1)}, \\ h &= \left(\frac{M+1}{M}x\right)^{Mn/(M+1)}, \\ (r')^2 &= 1 - \left(\frac{M+1}{M}x\right)^{2[M(1-n)-3]/(M+1)}. \end{aligned}\right\} \tag{35}$$

If we require the last of (35) to have as its last term the same power of x as the corresponding constant temperature equation (14), then (35) will describe the same body. In this manner, the relation of M to the body-shape parameter m and the temperature-variation index n is found to be

$$M = m \Big/ \left(1 - \frac{m+1}{4}n\right). \tag{36}$$

We observe from the last two of (35) that $h = 1$ at the upper extreme of the body; hence, the temperature difference at that point is the characteristic temperature difference and at other stations along the body it varies as a power of x. There is one limitation on this variation: The total heat convected from the body must be finite. One finds for the heat transfer over an extent x of the body

$$Q = -k(T_w - T_\infty)\, H'(0) \times \int_0^x \left(\frac{M+1}{M}x\right)^{(Mn-1)/(M+1)} \mathrm{d}x.$$

The requirement that the exponent in the integrand be greater than -1 specifies that n lie in the range

$$-1 < n < 4. \tag{37}$$

This is true for both ranges of body parameter, $m < -1$ and $m > 3$. Thus, there may be a singularity in the temperature at the tip of the contour, but not a strong one.

The temperature variation has the effect of rescaling the body. To illustrate this, we use the subscript max to designate the upper extreme of the body, substitute (37) into (35), and find

$$\left.\begin{aligned} x_{\max} &= M/(M+1) \\ &= m/(m+1)\,(1 - n/4) \\ &= [x_{\max}]_{n=0}/(1 - n/4), \\ z_{\max} &= [z_{\max}]_{n=0}/(1 - n/4), \\ r_{\max} &= [r_{\max}]_{n=0}/(1 - n/4), \\ L &= X_{\max}\frac{m+1}{m}(1 - n/4) \\ &= [L]_{n=0}(1 - n/4). \end{aligned}\right\} \tag{38}$$

Thus for a body of given size, the characteristic length changes by a factor $(1 - n/4)$ when the

temperature is varied. Through this modified characteristic length the Rayleigh number of the boundary layer responds to the change of temperature distribution.

The changes induced in boundary-layer thickness and velocity growth are found by substituting (36) into f and g of (35):

$$\left.\begin{aligned} f &= \left[\frac{(m+1)(1-n/4)}{m}\,x\right]^{\frac{m}{(m+1)(1-n/4)}}, \\ g &= \left[\frac{(m+1)(1-n/4)}{m}\,x\right]^{\frac{1-(m+1)n/4}{(m+1)(1-n/4)}}. \end{aligned}\right\} \quad (40)$$

The wall temperature distribution is given by

$$h = \left[\frac{(m+1)(1-n/4)}{m}\,x\right]^{\frac{m}{m+1}\,\frac{n}{1-n/4}}. \quad (41)$$

As an illustration of the effect of wall temperature distribution consider a vertical flat plate ($m = 3$). Let us see what temperature distribution is required to give the boundary layer the characteristics of those on the round-nosed body ($m = \infty$). In other words, we want to choose $M = \infty$. From equation (36), we find $n = 1$. Then

$$\left.\begin{aligned} f &= x, \\ g &= 1, \\ h &= x. \end{aligned}\right\} \quad (42)$$

Thus, a linear temperature gradient on a flat plate requires the boundary layer to grow as it would on a constant-temperature, round-nosed body. Of course, this not to say that the inner details—velocity and temperature profile—are the same; these can be markedly different.

Solutions of boundary-layer equations

The governing equations for the boundary layers on the system of bodies discussed above can be found by applying equations (11), (12) to (8), (9). The results are, under the restriction of constant wall temperature,

$$\frac{m-1}{m}(F')^2 - FF'' = \frac{\nu}{V^*L}F''' + \frac{\beta(T_w - T_\infty)GL}{(V^*)^2}H, \quad -Pr\,FH' = \frac{\nu}{V^*L}H''. \quad (43)$$

The body parameter m affects the equations only through one of the inertia terms. The behavior of the boundary layer is best examined separately for fluids of very large and very small Prandtl number.

The asymptotic formulation of the differential equations for large Pr has been made by Morgan and Warner [6] and by Braun and Heighway [1], we repeat the argument briefly. Because the fluid is very viscous, the velocity boundary layer is much thicker than the temperature boundary layer. However, for the purpose of heat transfer study, the latter is of principal interest. Therefore, a new co-ordinate normal to the wall is introduced,

$$\zeta = a\eta, \quad (44)$$

where a is to be chosen so that ζ is of order unity in the temperature layer and, therefore, derivatives taken with respect to it will also be of unit order. Introduction of (44) into (43) will thus bring the number of unspecified parameters in the equations to two: V^* and a. The physical conditions imposed to obtain them are: (1) the viscous forces in the thermal layer will be of magnitude comparable to the buoyancy forces, (2) the heat convection and the heat conduction terms must balance. It follows that

$$\left.\begin{aligned} V^* &= Ra^{1/4}\,a/L, \\ a &= Ra^{1/4}. \end{aligned}\right\} \quad (45)$$

The equations governing the boundary layer now become

$$Pr^{-1}\left(\frac{m-1}{m}F'^2 - FF''\right) = F''' + H, \quad (46a)$$

$$-FH' = H'', \quad (46b)$$

where primes signify differentiation with respect to ζ. At very large Prandtl numbers, the equations become nearly independent of the body parameter m.

The system (46) with boundary conditions

$$\left.\begin{aligned} F(0) &= F'(0) = F'(\infty) = 0, \\ H(0) &= 1, \qquad H(\infty) = 0, \end{aligned}\right\} \quad (47)$$

has been solved by the integral method described by Braun and Heighway [1]. The Nusselt number is found to be

$$Nu = \left[\frac{-L}{T_w - T_\infty}\frac{\partial T}{\partial Y}\right]_w = \frac{2}{\delta g} Ra^{1/4} \quad (48)$$

where g is the boundary-layer thickness given by (13) and δ is a number defining the edge of the thermal layer for the integral method. The latter is given by

$$\delta^4 = \frac{2^3 \cdot 3^2 \cdot 5 \cdot 7^2 \cdot 11 \cdot 13(1 + 3R)}{12294 + 19007R} \quad (49)$$

where R, in turn, is a measure of the ratio of temperature-layer thickness to velocity-layer thickness and is related to the Prandtl number by

$$Pr\, R^2 = \frac{2m - 1}{m}\frac{7 \cdot 11}{2^2 \cdot 3 \cdot 5 \cdot 17} \times \times \frac{55250 + 211623R + 533808R^2 + 304567R^3}{12294 + 19007R}. \quad (50)$$

The quantity $Nu\, g(x)/Ra^{1/4}$ has been plotted against Prandtl number for three of the two-dimensional bodies ($m = 3, \infty, -5$) in Fig. 2. The factor $g(x)$ in this quantity removes the effect of heat transfer variation along the wall of any body, thus facilitating a comparison between bodies. Physically, it shows that the heat transfer is greater in regions of the body where the boundary layer is thinner. Accordingly, on the flat bottomed bodies the heat transfer increases as one goes up the side, while on the pointed bodies it decreases. The rounded body ($m = \infty$) has a uniform heat transfer over all its surface. If the wall temperature varies, $g(x)$ is replaced by $g(x)/h(x)$. There is only a weak dependence of the heat transfer on the body-shape parameter m which, as predicted, disappears at large Prandtl numbers.

The situation prevailing at low Prandtl numbers is the reverse of that at high values [1]. The thermal layer extends much further into the fluid than the viscous layer. As the Prandtl number becomes very small, the medium behaves almost like an inviscid fluid. Again we make a transformation of the type (44) in the thermal layer and impose the conditions on (43) that (1) the inertia terms be of the same order of magnitude as the buoyancy force, and (2) heat conduction and convection balance. The parameters V^* and a for this case are determined to be

$$V^* = (Ra\, Pr)^{1/4}\, a/L, \quad (51)$$

$$a = (Ra\, Pr)^{1/4}. \quad (52)$$

The governing equations for the boundary layer are

$$\frac{m - 1}{m} F'^2 - FF'' = Pr\, F''' + H, \quad FH' = H'', \quad (53)$$

where primes now indicate differentiation with respect to

$$\zeta = (Ra\, Pr)^{1/4}\, \eta. \quad (54)$$

The boundary conditions are again (47). For

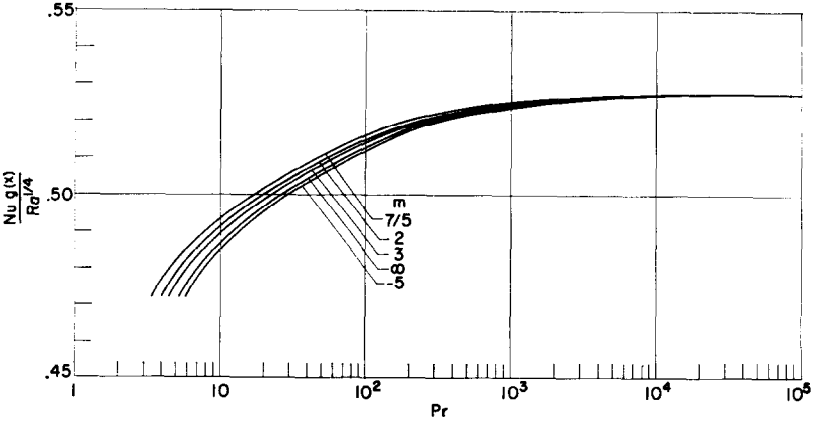

FIG. 2. Heat transfer on similarity bodies, high Prandtl number.

fluids with very small Prandtl numbers, the viscous term becomes negligible in the momentum equations (53).

According to the integral method [1] referred to above, the heat transfer is given by

$$\frac{Nu\, g(x)}{(Ra\, Pr)^{1/4}} = \frac{1}{\delta}\frac{3}{1+2r}. \tag{55}$$

The quantity δ describes the edge of the thermal layer for the integral method and is given by

$$\delta^4 = \left(\frac{2m-1}{m}\right)\frac{2^7\cdot 3^2\cdot 5}{7}\frac{(1+2r)(1+3r)}{(1+r)(1+3r^2)}\times \frac{70+126r+189r^2+230r^3+99r^4+54r^5}{(15+35r+65r^2+53r^3+24r^4)^2}. \tag{56}$$

The parameter r represents the ratio of the viscous-layer to thermal-layer thickness. It is related to the Prandtl number by

$$\frac{Pr}{r^2} = \left(\frac{2m-1}{m}\right)\frac{8}{7}\frac{1}{(1+r)(1+3r^2)}\times \frac{70+126r+189r^2+230r^3+99r^4+54r^5}{15+35r+65r^2+53r^3+24r^4}. \tag{57}$$

The quantity (55) is plotted against Pr in Fig. 3 for $m = 3, \infty, -5$. As anticipated from the differential equations (53), the effect of the body parameter m is greatest at very low Prandtl number where viscous effects are negligible. The integral method of solution used here is known to be least accurate at Prandtl numbers near one; therefore, solutions to the boundary value problem (53), (47) have been obtained on an electronic digital computer for Prandtl number 0·72. These computations are shown as triangles in Fig. 3. The two curves labeled $m = 7/5, 2$ and the corresponding machine computations refer to axisymmetric bodies to be discussed later.

AXISYMMETRIC BODIES

Similarity conditions

The equations describing the motion in a boundary layer over an axisymmetric body are identical in form with those over the two-dimensional body with the exception of the equation of continuity (1), which becomes

$$(UR_0)_X + (VR_0)_Y = 0. \tag{58}$$

One must now define the dimensionless stream function according to the relations

$$U = V^*\frac{1}{r}\psi_y, \quad V = -V^*\frac{1}{r}\psi_x. \tag{59}$$

$$\left.\begin{aligned} &\frac{f'}{f}(F'^2 - FF'') - \frac{(rg)'}{rg}(F')^2 \\ &= \frac{\nu}{V^*L}\frac{r}{fg}F''' \\ &+ \frac{\beta(T_w - T_\infty)GL}{V^{*2}}\sqrt{[1-(r')^2]}\left(\frac{rg}{f}\right)^2 H, \end{aligned}\right\} \tag{60}$$

and

$$-\frac{f'}{f}FH' = \frac{r}{fg}H''.$$

In each of equations (60) we have made a restriction to constant wall temperature by setting $h = 1$, $h' = 0$. Choosing the proportionalities

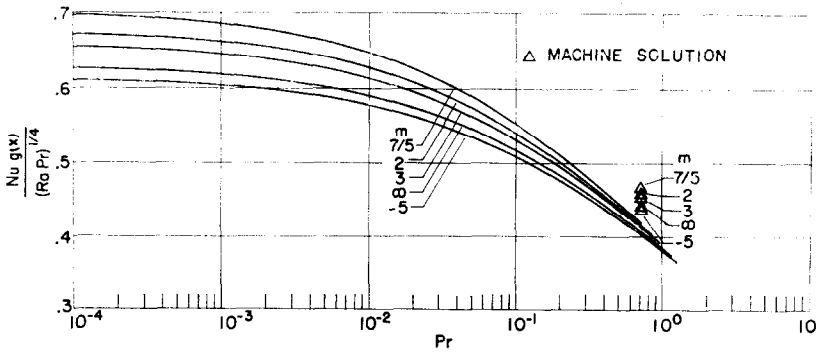

FIG. 3. Heat transfer on similarity bodies, low Prandtl number.

involving the stream function growth f, thickness g, and radius r to be

$$\frac{f'}{f} = m\frac{(rg)'}{rg} = \frac{r}{fg} = \sqrt{[1-(r')^2]}\left(\frac{rg}{f}\right)^2 \tag{61}$$

one has for the similar velocity and temperature distribution

$$\left.\begin{aligned} &\frac{m-1}{m}F'^2 - FF'' = \frac{\nu}{V^*L}F''' \\ &+\frac{\beta(T_w - T_\infty)GL}{(V^*)^2}H, \\ &\text{and} \\ &-FH' = \frac{\nu}{V^*L}H''. \end{aligned}\right\} \tag{43}$$

This is just the set (43) which was found previously for the two-dimensional flows.

The set (61), which determines the body shapes, is slightly more complicated than in the two-dimensional case, and the integration must proceed in a more *ad-hoc* manner. We can write

$$f = (rg)^m \tag{62}$$

but the body itself must be found before f and g can be specified.

Specific body shapes

Three axisymmetric bodies have been determined.

Cone. We begin by asking if there are any solutions that involve simple powers of x, as in the two-dimensional case. Setting

$$f = (ax)^k \tag{63}$$

one finds from (61) that

$$a = 0{\cdot}503555, \quad k = 7/4, \quad m = 7/5, \tag{64}$$

and

$$r = \sqrt{\left(\frac{7}{4}a^3\right)}\,x, \quad g = 2(49a)^{-1/4}\,x^{1/4}. \tag{65}$$

The first of (65) describes a cone of half-angle 28·210°. On it the boundary-layer thickness $g(x)$ grows at the same rate as that on a flat plate; likewise, the velocity growth, now given by f/rg, is proportional to that on the plate.

The exact value of the cone angle has not been left free here because the constants of proportionality in (61) have been arbitrarily chosen as unity in the second and third equations. It can be shown that if a cone has some other angle θ, the boundary-layer equations can be reduced to the form (43) by means of the transformation

$$\left.\begin{aligned} &F(\eta) = b\Phi(\xi), \\ &\eta = b\xi, \\ &b \equiv \frac{7}{4}\frac{\sin\theta}{(\cos\theta)^{3/2}}. \end{aligned}\right\} \tag{66}$$

The cone was first shown to be a body yielding similar flows by Merk and Prins [5].

Parabolic-nosed body. One sets $m = 2$ and obtains

$$f = (rg)^2, \quad f' = r/g, \quad f' = \sqrt{[1-(r')^2]}. \tag{67}$$

The third of (67) shows that

$$f(x) \equiv z(x). \tag{68}$$

Eliminating g, one has

$$f' = \sqrt{[1-(r')^2]}, \quad f = \frac{r^4}{1-(r')^2} \tag{69}$$

so that

$$\left(\frac{r^4}{1-(r')^2}\right)' = \sqrt{[1-(r')^2]}. \tag{70}$$

A first integral may be performed by using the identity

$$(r')^2 = \left[1+\left(\frac{\mathrm{d}z}{\mathrm{d}r}\right)^2\right]^{-1}. \tag{71}$$

Then

$$\left(\frac{\mathrm{d}z}{\mathrm{d}r}\right)^2 = \frac{r^4}{z-r^4}. \tag{72}$$

A series solution of the equation is

$$
\left.\begin{aligned}
z = f &= cr^2 + \tfrac{1}{5}r^4 + \frac{12}{7\cdot 5^2 c}r^6 \\
&\quad + \frac{2^4\cdot 13}{3^2\cdot 5^3\cdot 7c^2}r^8 \\
&\quad + \frac{2^6\cdot 163}{3\cdot 7^2\cdot 11\cdot 5^4 c^3}r^{10} + \cdots, \\
x &= r + \frac{1}{6c^2}r^3 + \frac{11c^2}{50}r^5 \\
&\quad + \frac{83}{4\cdot 5\cdot 7^2}r^7 + \frac{3067}{2^5\cdot 3^4\cdot 5\cdot 7c^2}r^9 \\
&\quad + \frac{11,726,851c^2}{2^4\cdot 3^2\cdot 5^4\cdot 7^2\cdot 11^2}r^{11} + \cdots, \\
c &= 4^{-1/3} = 0{\cdot}62996.
\end{aligned}\right\} \quad (73)
$$

It is seen that the body has a parabolic nose for which the dimensionless radius of curvature is

$$\rho = 1/2c$$

whence, if P is the dimensional radius of curvature at the nose, the characteristic length is

$$L = P/\rho = 2cP. \quad (74)$$

Flat-nosed body. Using (62) to eliminate f from the last of (61) yields

$$(rg)^{m-3} = \sqrt{[1 - (r')^2]}/r^2. \quad (75)$$

Choosing $m = 3$ eliminates g, and r is determined by

$$(r')^2 = 1 - r^4. \quad (76)$$

The solution of (76) in terms of a parametric angle φ is

$$
\left.\begin{aligned}
x &= 2^{-1/2}\,[F(45°, 90°) - F(45°, \varphi)], \\
z &= 2^{1/2}\,[E(45°, 90°) - E(45°, \varphi)] - x, \\
f &= (4z/3)^{3/4}, \quad r = \cos\varphi, \\
g &= f^{1/3}/r.
\end{aligned}\right\} \quad (77)
$$

The general features of the body are evident directly from the differential equation (76). The body is vertical ($r' = 0$) at $r = 1$. Its radius of curvature is given by

$$\rho = 1/2r \quad (78)$$

which becomes infinite at the origin, indicating that the body is flat on the bottom. From the first of (77), we also learn that $L = R_{\max}$.

Because $m = 3$ is also the value of the body parameter describing a flat plate, it is possible to use the solutions of the flow over the plate to describe the characteristics of the boundary layer on this axisymmetric body.

The three axisymmetric bodies that have been derived here—the cone, the parabolic-nosed body, the flat-nosed body—are shown together on Fig. 4. The functions $f(x)$, $g(x)$, $r(x)$ are

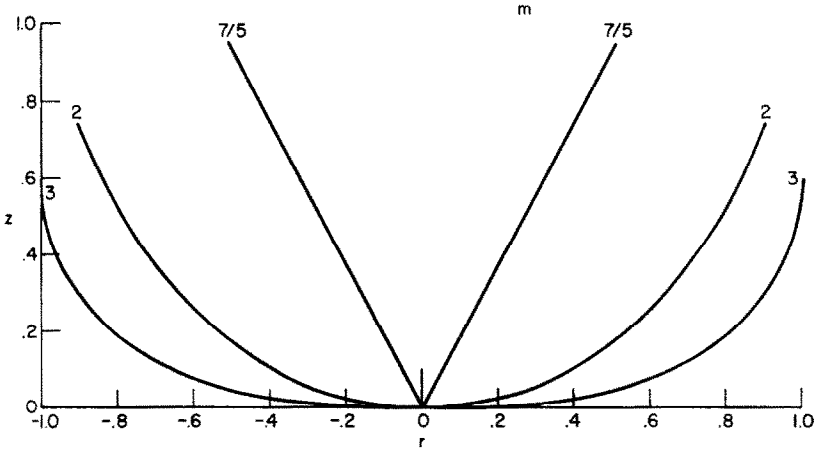

FIG. 4. Axisymmetric similarity bodies.

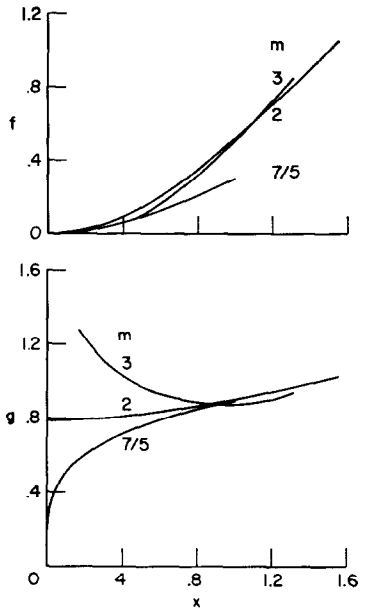

FIG. 5. Boundary-layer growth functions on axisymmetric similarity bodies.

shown in Fig. 5. It is evident from the plot of $g(x)$ that the boundary-layer assumption does not hold at the nose of the body $m = 3$.

Heat transfer on axisymmetric bodies

Equations (43) for the flow over the axisymmetric bodies described by $m = 7/4, 2, 3$ have been solved by the integral method referred to previously. At large Prandtl numbers the local heat transfer is given by equation (48). It has been plotted along with the curves for the two-dimensional bodies in Fig. 2. The curve for $m = 3$, of course, represents the flat plate as well as the flat-bottomed body. Again, the effect of body shape is not strong.

The nondimensional local heat transfer at low Prandtl numbers is given by (55) and is shown in Fig. 3, along with curves for the two-dimensional bodies. The body shape influences the heat transfer most strongly at the very low Prandtl numbers.

Solutions obtained by machine integration of the equations at $Pr = 0{\cdot}72$ are included in the figure.

FLOW OVER CIRCULAR CYLINDER

We will now illustrate the use of the body contours and their corresponding flows to obtain the flows of "nearby" bodies. The body $m = \infty$ has a finite and nonzero radius of curvature everywhere, and may, therefore, be used as a zeroth approximation to the lower portion of a horizontal circular cylinder. Higher approximations may be obtained by an iteration process.

When the radius of curvature at the bottom is taken as the characteristic length, the radical appearing in the buoyancy term for the $m = \infty$ body is

$$\sqrt{[1 - (r'_\infty)^2]} = x. \tag{79}$$

The circular cylinder has a radius described by

$$r = \sin x \tag{80}$$

and hence

$$\sqrt{[1 - (r')^2]} = \sqrt{[1 - (r'_\infty)^2]}\,(1 - x^2/6 + \ldots). \tag{81}$$

Making the restriction to constant wall temperature and small Prandtl numbers, one has

$$f = x, \quad g = 1, \quad h = 1, \quad \zeta = (Ra\,Pr)^{1/4}\,y. \tag{82}$$

Perturbations of the stream function and temperature profile are made by setting

$$\left.\begin{aligned} F &= F_0 + x^2 F_1 + \ldots \\ H &= H_0 + x^2 H_1 + \ldots . \end{aligned}\right\} \tag{83}$$

Then the equations (8) and (9) governing the boundary layer become, to zero order in x^2,

$$\left.\begin{aligned} (F'_0)^2 - F_0 F''_0 &= Pr\,F'''_0 + H_0, \\ -F_0 H'_0 &= H''_0, \end{aligned}\right\} \tag{84}$$

and to first order in x^2,

$$\left.\begin{aligned} 4F'_1F'_0 - F_0F''_1 - 3F_1F''_0 & \\ = Pr\,F'''_1 + H_1 - \frac{1}{6}H_0, & \\ 2F'_0H_1 - F_0H'_1 - 3F_1H'_0 = H''_1. & \end{aligned}\right\} \tag{85}$$

The boundary conditions accompanying (84) and (85) are

$$\left.\begin{aligned} H_0(0) &= 1, \quad H_0(\infty) = 0, \\ F_0(0) &= 0, \quad F'_0(0) = 0, \quad F'_0(\infty) = 0, \end{aligned}\right\} \tag{86}$$

and

$$\left.\begin{aligned} &H_1(0) = 0, \quad H_1(\infty) = 0, \\ &F_1(0) = 0, \quad F_1'(0) = 0, \quad F_1'(\infty) = 0. \end{aligned}\right\} \quad (87)$$

In integral form, (84) and (85) become

$$\left.\begin{aligned} &2\int_0^\delta (F_0')^2 \, d\zeta = \int_0^\delta H_0 \, d\zeta - Pr\, F''(0), \\ &\int_0^\delta F_0' H_0 \, d\zeta = -H_0'(0), \end{aligned}\right\} \quad (88)$$

and

$$\left.\begin{aligned} &8\int_0^\delta F' F_0' \, d\zeta \\ &\quad = \int_0^\delta \left(H_1 - \frac{1}{6} H_0\right) d\zeta - Pr\, F_1''(0), \\ &3\int_0^\delta (F_0' H_1 + F_1' H_0) \, d\zeta = H'(0). \end{aligned}\right\} \quad (89)$$

Equations (88) are among those already solved in a preceding section.

In the limiting case $Pr = 0$, one may use very simplified velocity profiles to solve equations (88) and (89). We allow the fluid to slip at the wall and write

$$\left.\begin{aligned} &F_0' = A(1 - \zeta/\delta)^4, \\ &F' = (-1/24 + b\zeta/\delta)(1 - \zeta/\delta)^4. \end{aligned}\right\} \quad (90)$$

The constant $-1/24$ appearing in the perturbation velocity is determined by evaluating the second of the differential equations (85) at $\zeta = 0$. Likewise, we write

$$\left.\begin{aligned} &H_0 = (1 - \zeta/\delta)^3, \\ &H_1 = (c\zeta/\delta + d(\zeta/\delta)^2)(1 - \zeta/\delta)^3. \end{aligned}\right\} \quad (91)$$

The second of the differential equations (85) evaluated at $\zeta = 0$ requires

$$3c = d. \quad (92)$$

The zero order integral equations (88) determine A and δ.

$$\left.\begin{aligned} &A = 3/[2\sqrt{(2)}], \\ &\delta = 4 \cdot 2^{1/4}. \end{aligned}\right\} \quad (93)$$

The first order integral equations (89) yield

$$\left.\begin{aligned} &b = \frac{175}{27 \cdot 16}\left(1 - \frac{39}{25\sqrt{(2)}}\right) = -0{\cdot}04173, \\ &d = \frac{25}{72}[1 - \sqrt{(2)}/15] = 0{\cdot}3145. \end{aligned}\right\} \quad (94)$$

Having found all the constants defining the polynomials, one can determine the heat transfer from the derivatives of (91). The local Nusselt number is given by

$$Nu(Ra\, Pr)^{-1/4} = 0{\cdot}631\,(1 - 0{\cdot}0349x^2). \quad (95)$$

The heat transfer is seen to reduce as one moves up the side of the cylinder. The Nusselt number expression (95) holds only for $x^2 \leq 1$ because the $m = \infty$ body is not defined beyond this limit. Merk and Prins [5] have computed the heat transfer over the entire cylinder by assuming a similarity flow. Strictly, this is not correct; however, in our notation their result at $Pr \to 0$ is

$$Nu(Ra\, Pr)^{-1/4} = 0{\cdot}528\,(1 - x^2/26 + \ldots) \quad (96)$$

in which the correction term is in good agreement with (95). Although Merk and Prins carry (96) out to many more terms, it does not correctly describe the heat transfer on the upper half of the cylinder. This failure is evidently connected with the fact that the zero-order solution (the flow on the $m = \infty$ body) extends only part of the way up the cylinder.

CONCLUDING REMARKS

The effect of body shape on the heat transfer curves arises from the appearance of the body parameter m in the equations of motion (43). The only effect is on one inertia term by a factor $(m - 1)/m$. Table 1 shows

Table 1. *Inertia-term coefficient*

m	7/5	2	3	∞	-5
$\frac{m-1}{m}$	2/7	1/2	2/3	1	6/5

that as the bodies become flatter (m increases), inertia effects become more important. Corresponding to this is a slight lowering of the successive heat transfer curves in Figs. 2 and 3.

Merk and Prins used the integral method of Saunders to obtain heat transfer on the surfaces of the cone and the flat plate and at the lower stagnation points of the circular cylinder and the sphere. The heat transfer at the bottom of a cylinder or sphere corresponds to that from the present $m = \infty$ or $m = 2$ bodies, respectively. It was not necessary for Merk and Prins to find the bodies themselves in order to solve the corresponding boundary-layer equations. Some of their results in the low Prandtl number range are given in Table 2:

Table 2. Heat transfer at low Prandtl number

		$Nu\,g(x)\,(Ra\,Pr)^{-1/4}$			
	Pr	$m = 7/5$	$m = 2$	$m = 3$	$m = \infty$
Merk and Prins	0·0	∞	0·762	0·661	0·564
	0·72	0·458	0·444	0·435	0·424
Machine	0·72	0·467	0·458	0·452	0·441

Comparison of the first row of the table with Fig. 3 shows that the Merk and Prins computations indicate a much stronger effect of body shape than do ours. The method breaks down for the cone ($m = 7/5$) and gives the wrong dependence on Prandtl numbers in the low Prandtl number range. From the last two lines of the table one obtains a very satisfactory agreement between the Merk and Prins computations and the machine results shown as triangles in Fig. 3. If we increase Pr further to very large values, the Merk and Prins calculations give, in our notation,

$$Nu\,g(x)\,Ra^{-1/4} = 0{\cdot}422.$$

This is considerably lower than the value 0·528 given in Fig. 2. We conclude that the method of Saunders used by Merk and Prins, while accurate for Prandtl numbers of order unity, may not be so reliable at extremes of Prandtl number.

Schuh has also given a solution for the round cylinder ($m = \infty$) at $Pr = 0{\cdot}7$. This is a numerical computation yielding

$$Nu\,g(x)\,(Ra\,Pr)^{-1/4} = 0{\cdot}442,$$

which is in close agreement with our own machine solution at $Pr = 0{\cdot}72$.

REFERENCES

1. W. H. Braun and J. E. Heighway, *An Integral Method for Natural Convection Flows at High and Low Prandtl Numbers.* NASA TN D-292 (1960).
2. E. R. G. Eckert, *Introduction to the Transfer of Heat and Mass.* Second edition, McGraw-Hill, New York (1959).
3. V. M. Falkner and Sylvia W. Skan, *Some Approximate Solutions of the Boundary Layer Equations.* A.R.C. Reports and Memoranda No. 1314 (1930).
4. S. Goldstein (Editor), *Modern Developments in Fluid Dynamics.* Vol. 1, Oxford University Press, Oxford (1938).
5. H. J. Merk and J. A. Prins, *Appl. Sci. Res.* A **4**, pt. I, 11, pt. II, 195; pt. III, 207 (1953–54).
6. George W. Morgan and W. H. Warner, *J. Aero. Sci.* **23**, 937 (1956).
7. Simon Ostrach, *An Analysis of Laminar Free-Convection Flow and Heat Transfer About a Flat Plate Parallel to the Direction of the Generating Body Force.* NACA Rep. 1111 (1953).
8. H. Schuh, *Boundary Layers of Temperature.* Reports and Translations No. 1007 (1948).
9. E. M. Sparrow and J. L. Gregg, *Trans. Amer. Soc. Mech. Engrs.* **80**, 879 (1958).
10. K. Stewartson *Z. Angew. Math. Phys.* **9a**, (3), 276 (1958).